CHAPTER-V

SIMILARITY SOLUTIONS OF A STRONG SHOCK WAVE PROPAGATION IN A MIXTURE OF A GAS AND DUSTY PARTICLES UNDER THE INFLUENCE OF MONOCHROMATIC RADIATION

5.1 INTRODUCTION:

The study of shock waves in a mixture of a gas and small solid particles is of great importance due to its applications to many astrophysical problems. Pai et al. [42] have generalized the well known solution of a point explosion in gas (Sedov [58], Korobeinikov [23]) to the case of two phase flow of a mixture of a gas and small particles and brought out the essential effects due to the presence of dusty particles on such a strong shock wave. Subsequently, many papers on strong wave propagation in a mixture of gas and dusty particles appeared in the literature as that of Steiner and Hirschler [67], Vishwakarma and Pandey [77], Vishwakarma and Nath [75]. Later, radiation effect was introduced to the case of two phase flow of a mixture of a gas and small solid particles. Vishwakarma and Vishwakarma [78] generalized the work of Ashraf and Sachdev [3] by introducing radiation heat flux; Singh and Vishwakarma [65] generalized the work of Vishwakarma [73] by taking radiation flux into account, Vishwakarma and Nath [76] obtained self-similar solution by taking heat conduction and radiation heat flux.

Sedov [58] developed certain class of self-similar solution of the problem of the motion of gas with a distributed nature of the energy release. These self-similar solutions have been used by Khudyakov [21] (cf Nath [32]) to discuss the problem of the motion of gas under the action of monochromatic radiation.

Khudyakov [21] has considered that a homogeneous gas at rest occupies a half-space bounded by a fixed plane wall and assumed that a radiation flux moves through the gas in the direction of the wall with constant intensity per unit area and a shock wave that propagates out from the wall in a direction opposite to the

direction of the radiation flux from the instant of arrival of the radiation at the wall. He assumed also that the energy is absorbed only in the zone between the shock wave and the wall and that part of the incident radiation flux that has reached the wall passes through the wall without interacting through it. Onkar Nath [32] Studied the theoretical model of cylindrical MHD shock wave under the action of monochromatic radiation (see also Ganguly and Jana [13]). In this paper, we have examined one dimensional unsteady self similar adiabatic flow of a dusty gas behind a spherical shock wave with time dependent energy input and the radiation heat flux with constant intensity is moving in the opposite direction to the propagation of the shock wave. The dusty gas is assumed to be a mixture of small solid particles and a perfect gas. Since we have taken absorption coefficient independent of frequency of radiation, i.e. for mathematical simplicity, the approximation that is made for such an assumption is called grey body approximation (Basu [4]). Again due to the process of opacity limited fragmentation, gas in the present case is the considered as grey and opaque for the study of shock waves (Basu [4]).

We may assume that the viscous stress and heat conduction of the mixture of the gas and small particles are negligible (Pai et al. [42]). Furthermore, the solid particles are considered as a pseudo-fluid and it is assumed that the equilibrium condition is maintained in flow fluid so that the velocity of the gas, that the pseudo-fluid of the solid particles, and that of the mixture are equal. The temperature of the gas, that of the solid particles, and that of the mixture are also equal.

5.2 FUNDAMENTAL EQUATIONS AND BOUNDARY CONDITIONS:

The equations of motion for spherically symmetric one-dimensional unsteady flow of mixture of a gas and small solid particles under the influence of monochromatic radiation is given by (Pai et al. [42])

$$\frac{\partial \rho}{\partial t}+u\frac{\partial \rho}{\partial r}+\frac{\rho}{r^2}\frac{\partial}{\partial r}\left(u.r^2\right)=0, \tag{1}$$

$$\frac{\partial u}{\partial t}+u\frac{\partial u}{\partial r}+\frac{1}{\rho}\frac{\partial p}{\partial r}=0, \tag{2}$$

$$\frac{\partial U_m}{\partial t}+u\frac{\partial U_m}{\partial r}-\frac{p}{\rho^2}\left(\frac{\partial \rho}{\partial t}+u\frac{\partial \rho}{\partial r}\right)-\frac{1}{\rho r^2}\frac{\partial}{\partial r}\left(jr^2\right)=0, \tag{3}$$

$$\frac{\partial j}{\partial r}=Kj \tag{4}$$

where

ρ, u, p , U_m, r, j, t is the density of the mixture, the flow velocity, the pressure of the mixture, the internal energy per unit mass of the mixture, the radial distance, monochromatic radiation flux , the time respectively.

The monochromatic radiation flux term in equation (3) has been introduced following Nath [30], Ganguly and Jana [13] and K in (4) is the absorption coefficient which is considered as Nath [21]

$$K=K_0\rho^n p^m j^q r^s t^l, \tag{5}$$

where the dimensions of the constant coefficient are given by

$$\left[K_0\right]=M^{-n-m-q}L^{3n+m-s}T^{2m+3q-l}. \tag{6}$$

Moreover, the dimensional constants J_0, p_0, ρ_0 are related as,

$$J_0=p_0^{3/2}\rho_0^{-1/2}. \tag{7}$$

The equation of the state of the mixture can be written as (Pai et al.[42], Jena and

Sharma [20])

$$p = \frac{(1-k_p)}{1-Z}\rho R^* T, \tag{8}$$

where k_p is the mass concentration of the solid particles in the mixture, Z is the volume fraction of the solid particles, R* is the gas constant and T is the temperature of the mixture.

The density of the mixture as a whole is given by Pai et al.[42]

$$\rho = Z\rho_{sp} + (1-Z)\rho_g, \tag{9}$$

where ρ_{sp} is the species density of the solid particles and ρ_g the species density of the gas. The relation between Z and k_p is as follows:

$$k_p = \frac{Z\rho_{sp}}{\rho}. \tag{10}$$

In the equilibrium flow, k_p is the constant in the whole flow field.

The internal energy of the mixture U_m may be written as

$$U_m = \left[k_p c_{sp} + (1-k_p)c_v\right]T = c_{vm}T, \tag{11}$$

where c_{sp} is the specific heat of the solid particles, c_v is the specific heat of the gas at constant volume and c_{vm} is the specific heat of the mixture at constant volume.

The specific heat of the mixture at constant pressure c_{pm} is given by

$$c_{pm} = k_p c_{sp} + (1-k_p)c_p, \tag{12}$$

where c_p is the specific heat of the gas at constant pressure process.

The ratio of the specific heats of the mixture is

$$\Gamma = \frac{c_{pm}}{c_{vm}} = \gamma\frac{(1+\delta\beta'/\gamma)}{1+\delta\beta'}, \tag{13}$$

where $\gamma = c_p/c_v$, $\delta = k_p/(1-k_p)$ and $\beta' = c_{sp}/c_v$.

The internal energy of the mixture is therefore given by [using eq. (11), (12) and (13)]

$$U_m = \frac{p(1-Z)}{\rho(\Gamma-1)}. \qquad (14)$$

We consider that a strong spherical shock is propagating into the mixture of perfect gas and small solid particles of constant density at rest. Therefore,

$\rho_0 =$ constant and $u_0 = 0$,

where sub script "0" refers to the value in front of the shock. The total energy of the flow field behind the shock is not constant, but assumed to be time dependent and varying as Rogers [50]

$$E = E_C t^m \qquad (m \geq 0), \qquad (15)$$

where, E_c and m are constants. This class of flows includes the instantaneous constant energy blast wave, which is given by the value m=0. Furthermore, attention is confined to positive values of m only, that is, to those cases in which the total energy increases with time. Since the shock is strong, this increase can only be achieved by the pressure exerted on the fluid by an expanding surface (a contact surface or a piston).Thus the flow is headed by a shock front and has an expanding surface as an inner boundary.

The jump conditions across the shock are as follows:

$$u_2 = (1-\beta)\dot{R},$$

$$\rho_2 = (\rho_0/\beta),$$

$$p_2 = (1-\beta)\rho_0 \dot{R}^2 ,$$

$$Z_2 = (Z_0 / \beta) , \qquad (16)$$

where $\dot{R} = dR/dt$ denotes the shock velocity, R is the shock radius, and subscript "2" refers to the value just behind the shock. The quantities β and Z_0 given by the relations (Pai et al. [42], Steiner and Hirschler [67])

$$\beta = \frac{\Gamma - 1 + 2Z_0}{\Gamma + 1} \qquad \text{and} \qquad Z_0 = \frac{k_p}{G(1-k_p)+k_p} , \qquad (17)$$

where $G = \rho_{sp} / (\rho_g)_0$ is the ratio of the density of solid particles to the initial density of the gas. The particular case G=1 is associated with $Z_0 = k_p$. Also Z_0 being the initial volume fraction of solid particles is responsible for loss of compressibility of the dusty gas.

5.3 SIMILARITY SOLUTIONS:

By the standard dimensional analysis of Sedov [58], the non dimensional variable η is defined by

$$\eta = \left(\frac{\rho_0}{\nu E_c}\right)^{\frac{1}{5}} r t^{-\lambda} , \qquad (18)$$

where $\lambda = (2+m)/5$ and the parameter ν is taken so that η takes the value 1 at the shock surface. This discloses that η = r/R. The position of the inner expanding surface is given by $\eta = \bar{\eta}(= \bar{r}/R)$.

From relation (18), it follows that the motion of the shock front is described by the equation

$$\dot{R} = \lambda \left(\frac{\rho_0}{\nu E_c} \right)^{-\frac{1}{5}} t^{(m-3)/5}. \tag{19}$$

From this relation it can be seen that the value m = 3 corresponds to uniform expansion of a spherical shock. Therefore, the solutions of physical significance appear to be those for which m lies in the range 0 to 3.

We introduce the following transformation for finding out the similarity solutions.

$$U = (r/t)U(\eta), \tag{20}$$

$$\rho = \rho_0 D(\eta), \tag{21}$$

$$p = \rho_0 (r^2/t^2) P(\eta), \tag{22}$$

$$j = \rho_0 (r^3/t^3) J(\eta). \tag{23}$$

Making use of these transformations, the equations of motion (1) to (4) governing the one dimensional unsteady flow behind the shock wave can be transformed into the following set of ordinary differential equations:

$$\eta \left[(\lambda - U)\frac{D'}{D} - U' \right] = 3U, \tag{24}$$

$$\eta \left[(\lambda - U)U' - \frac{P'}{D} \right] = \left[U(U-1) + \frac{2P}{D} \right], \tag{25}$$

$$\eta(\lambda - U)\left[\frac{P'}{P} - \frac{D'}{D} - \frac{D'Z_0}{(1-Z_0D)} - \frac{(\Gamma-1)}{(1-Z_0D)}\frac{D'}{D} + \frac{(5J + J'\eta)(\Gamma-1)}{P(1-Z_0D)} \right] = 2(U-1), \tag{26}$$

$$J' = \alpha \eta^s D^n P^m J^{q+1}, \tag{27}$$

where prime denotes differentiation with respect to η.

From equations (24) to (27), we get

$$U' = \frac{\frac{P}{\eta}\left[\frac{-2(U-1)}{D} + \frac{1}{P}(\lambda - U)\left\{-U(U-1) - \frac{2P}{D}\right\} - 3LU + \frac{(5J + J'\eta)(\Gamma - 1)}{DP(1 - Z_0 D)}\right]}{\left[LP - (\lambda - U)^2\right]},$$

(28)

$$P' = \frac{\left[(\lambda - U)\frac{DP}{\eta}\left\{\frac{-2(U-1)}{D} + \frac{1}{P}(\lambda - U)\left\{-U(U-1) - \frac{2P}{D}\right\} - 3LU + \frac{(5J + J'\eta)(\Gamma - 1)}{DP(1 - Z_0 D)}\right\}\right]}{\left[LP - (\lambda - U)^2\right]}$$

$$- \frac{DU(U-1)}{\eta} - \frac{2P}{\eta}, \qquad (29)$$

$$D' = \frac{3DU}{(\lambda - U)\eta} + \frac{\frac{DP}{\eta}\left[\frac{-2(U-1)}{D} + \frac{1}{P}(\lambda - U)\left\{-U(U-1) - \frac{2P}{D}\right\} - 3LU + \frac{(5J + J'\eta)(\Gamma - 1)}{DP(1 - Z_0 D)}\right]}{(\lambda - U)\left[LP - (\lambda - U)^2\right]}$$

(30)

$$J' = \alpha \eta^s D^n P^m J^{q+1}, \qquad (31)$$

where,

$$L = \frac{1}{D} + \frac{Z_0}{(1 - Z_0 D)} + \frac{(\Gamma - 1)}{(1 - Z_0 D)D}$$

The shock conditions are transformed into the following form:

$$U(1) = (1 - \beta)\lambda,$$

$$D(1) = 1/\beta,$$

$$P(1) = (1 - \beta)\lambda^2,$$

$$J(1) = (1 - \beta)\lambda^3 \qquad (32)$$

The condition to be satisfied at the inner expanding surface is that the velocity of the fluid is equal to the velocity of the surface itself. This kinematics condition, from equations (18) and (20), can be written as:

$$U(\eta) = \lambda \tag{33}$$

With the help of equations (20)-(23) and (32), the solutions can be written in the following convenient form:

$$\frac{u}{u_2} = \frac{\eta}{(1-\beta)\lambda} U(\eta), \tag{34}$$

$$\frac{Z}{Z_2} = \frac{\rho}{\rho_2} = \beta D(\eta), \tag{35}$$

$$\frac{p}{p_2} = \frac{\eta^2}{\lambda^2(1-\beta)} P(\eta), \tag{36}$$

$$\frac{j}{j_2} = \frac{\eta^3}{\lambda^3(1-\beta)} J(\eta) \tag{37}$$

where $U(\eta)$, $D(\eta)$, $P(\eta)$ and $J(\eta)$are obtained from numerical integration of the set of ordinary differential equations (28)-(31).

Because of the dependence of the boundary conditions (32) and equations (28)-(31) on the initial volume of the solid particles Z_0, a similarity solution exists only when Z_0 is constant, i.e., when the initial density ρ_0 of the mixture is constant. Therefore, the problem of two phase flow is different from that of a perfect gas. In the latter case, a similarity solution exists even when the initial density varies as some power of distance (Sedov [58], Rogers [48]).

5.4 NUMERICAL RESULTS AND DISCUSSIONS:

We have integrated equations (28)-(31) numerically by using the forth order Runge-Kutta method for the values of constants α =5.0, n=-1/2, q=0, s=1,

m=3/2. The integration began at η =1 with the boundary conditions (32) and terminated at $\eta = \lambda$ which corresponds to the center of symmetry. In our numerical results, the following non-dimensional parameters are used

γ = 1.3; 1.4; 2.0; 3.0; 6.0;

k_p = 0.1; 0.4; 0.6;

G = 1; 10; 100.

Some of the typical results are presented below.

In Figs.(1)-(4) and from Table 1, the effects of γ are given. We observe that fluid velocity u/u_2 is higher at the inner expanding surface than at the shock front for γ = 1.3, 1.4, & 2.0, but it is decreases for the γ = 3.0, & 6.0.The fluid velocity of inner expanding surface being higher than the fluid velocity just behind the shock may be due to increasing input for m = 1.75 in equation (15).

In Fig. (2) the density ρ/ρ_2 increases abruptly except for the case of γ = 1.3 where it tends to decrease then at the end, it increases slightly as we move towards the centre of shock. Further, as γ changes from 1.3 to 6.0, there is a rapid increase in the value of density. In Fig.3, the pressure tends to decrease as we move towards the centre of the shock except for the cases γ = 1.3 and γ = 1.4. While for γ = 1.4, there is an abrupt increase in pressure, for γ = 1.3 the pressure first decreases and then show slight increasing trend as one goes towards the centre of shock. Further for higher values of γ from 2.0 to 6.0, the pressure decreases as we go towards the centre of shock. Finally, in Fig.4, monochromatic radiation j/j_2 decreases steadily for all values of γ as we move towards the centre of the shock. However as we move upwards from origin on j/j_2 excesses of the

graph this fall decreases from lower value towards higher value.

In Fig. 5-8 and from Table 2, the effects of k_p and G are given. For $\gamma = 1.4$ and G=1, Fig.5 shows that the velocity u/u_2 increases with the increase of k_p. For k_p =0.6; the value increases as G increases except for G=100, it increases and then suddenly decreases abruptly. In Fig.6 we find for $\gamma = 1.4$ and G=1, the density decreases with increase of k_p but for large G such as G=100 the density increase with increase of G. Fig.7 shows variation of pressure. For $\gamma = 1.4$ and G=100 or larger, pressure increases with increase of k_p . In Fig 8, we find that for $\gamma = 1.4$, G=1 monochromatic radiation decrease slowly as we go towards the centre of the shock except for $k_p = 0.6$, G=100 where it abruptly decreases.

In Figs. 9-10 and Table 3, the effects of m and G are given. In Fig.9, with $\gamma = 1.4$ and $k_p = 0.6$ we show the variation of velocity u/u_2 with eta at various energy E for different values of m (in ergs/cm^2) (eq. 15) and various G, in general the velocity increases with E but decreases with G, notably at G=100. In Fig.10, we observe the variation of density for a given $\gamma = 1.4$ and k_p =0.6 but different values of E and G. For G=100, the density increases abruptly for m = 1.75. Again for m=1.5, G=100 density decreases. Same feature in variation of pressure in Fig.11. In Fig.12, the monochromatic radiation decreases towards the centre of the shock. But the case m=1.75 and G=100; are different from other value of m and G. Again a curious thing is showed in Fig.8 and 12. The variation of monochromatic radiation due to k_p =0.6 in Fig.8 and the variation of monochromatic radiation due to m=1.75 in Fig.12 are same of the values of G=100. Thus m and k_p have the same role in variation of monochromatic radiation.

Table 1: The Numerical variation of flow variables with variation of γ.

	η	γ=1.3	γ=1.4	γ=2.0	γ=3.0	γ=6.0
u	0.75	1.68	0.98	1.27	0.82	0.72
	0.80	1.72	0.84	1.14	0.88	0.83
	0.85	1.34	1.27	1.03	0.89	0.89
	0.90	1.16	1.12	0.97	0.87	0.77
	0.95	1.05	1.03	0.95	0.89	0.83
	1.00	1.00	1.00	1.00	1.00	1.00
ρ	0.75	2.09	5.34			
	0.80	1.62	4.07			
	0.85	1.93	2.41	7.52		
	0.90	1.81	2.13	4.94		
	0.95	1.47	1.62	2.52	3.97	7.40
	1.00	1.00	1.00	1.00	1.00	1.00
p	0.75	1.18	2.43	0.82	0.75	0.34
	0.80	0.84	2.26	1.13	0.95	0.47
	0.85	1.15	1.18	1.26	1.15	0.54
	0.90	1.16	1.17	1.22	1.23	1.01
	0.95	1.09	1.10	1.12	1.14	1.16
	1.00	1.00	1.00	1.00	1.00	1.00
j	0.75	0.38	0.34	0.53	0.67	0.79
	0.80	0.45	0.46	0.56	0.68	0.79
	0.85	0.52	0.54	0.61	0.69	0.79
	0.90	0.64	0.65	0.69	0.74	0.79
	0.95	0.79	0.79	0.81	0.82	0.84
	1.00	1.00	1.00	1.00	1.00	1.00

Table 2: The Numerical variation of flow variables with variation of k_p & G with similarity parameter η.

	x	k_p =0.1			k_p =0.4			k_p =0.6		
		G=1	G=10	G=100	G=1	G=10	G=100	G=1	G=10	G=100
u/u_2	0.75	0.98		1.67	1.29			2.18		-3.20
	0.80	0.84	1.64	1.69	1.64		1.61	1.72	1.68	-3.03
	0.85	1.27	1.27	1.27	1.37	1.38	1.38	1.44	1.47	1.49
	0.90	1.12	1.11	1.11	1.19	1.18	1.17	1.24	1.23	1.23
	0.95	1.03	1.03	1.03	1.07	1.06	1.06	1.10	1.09	1.09
	1.00	1.00	1.00	1.00	1.00	1.00	1.00	1.00	1.00	1.00
ρ/ρ_2	0.75	5.34		2.43	2.61			1.39		8.63
	0.80	4.07	1.96	1.83	1.78		1.70	1.49	1.43	7.72
	0.85	2.41	2.44	2.44	1.77	1.78	1.77	1.46	1.42	1.40
	0.90	2.13	2.17	2.18	1.64	1.71	1.73	1.39	1.44	1.46
	0.95	1.62	1.63	1.63	1.38	1.42	1.43	1.25	1.29	1.30
	1.00	1.00	1.00	1.00	1.00	1.00	1.00	1.00	1.00	1.00
p/p_2	0.75	2.43		1.05	1.99			0.47		9.75
	0.80	2.26	0.81	0.74	1.00		1.04	1.00	1.06	7.32
	0.85	1.18	1.18	1.18	1.15	1.13	1.13	1.13	1.09	1.07
	0.90	1.17	1.18	1.18	1.15	1.15	1.15	1.13	1.13	1.13
	0.95	1.10	1.10	1.10	1.09	1.09	1.09	1.08	1.08	1.08
	1.00	1.00	1.00	1.00	1.00	1.00	1.00	1.00	1.00	1.00
j/j_2	0.75	0.34		0.42	0.34			0.36		0.06
	0.80	0.46	0.47	0.47	0.43		0.44	0.41	0.42	0.23
	0.85	0.54	0.54	0.54	0.51	0.52	0.52	0.50	0.50	0.50
	0.90	0.65	0.65	0.65	0.63	0.63	0.63	0.62	0.62	0.62
	0.95	0.79	0.79	0.79	0.79	0.79	0.79	0.78	0.79	0.79
	1.00	1.00	1.00	1.00	1.00	1.00	1.00	1.00	1.00	1.00

Table 3: The Numerical variation of flow variables with variation of m & G with similarity parameter η.

	x	m=0.5			m=1.5			m=1.75		
		G=1	G=10	G=100	G=1	G=10	G=100	G=1	G=10	G=100
u/u_2	0.75	2.29	1.57	-0.43	2.15	2.36	3.10	2.18		-3.2
	0.80	2.20	1.46	1.63	1.73	2.30	1.26	1.72	1.68	-3.03
	0.85	1.46	1.43	1.70	1.44	1.48	1.51	1.44	1.47	1.49
	0.90	1.24	1.23	1.22	1.24	1.23	1.22	1.24	1.23	1.23
	0.95	1.09	1.08	1.07	1.10	1.09	1.08	1.10	1.09	1.09
	1.00	1.00	1.00	1.00	1.00	1.00	1.00	1.00	1.00	1.00
ρ/ρ_2	0.75	1.03	1.46	4.25	1.32	0.74	-0.6	1.39		8.63
	0.80	0.84	1.38	1.15	1.40	0.59	1.88	1.49	1.43	7.72
	0.85	1.23	1.21	0.90	1.40	1.34	1.30	1.46	1.42	1.40
	0.90	1.21	1.23	1.24	1.33	1.38	1.40	1.39	1.44	1.46
	0.95	1.13	1.16	1.17	1.21	1.25	1.26	1.25	1.29	1.30
	1.00	1.00	1.00	1.00	1.00	1.00	1.00	1.00	1.00	1.00
p/p_2	0.75	0.14	1.28	4.26	0.50	0.36	-0.84	0.47		9.75
	0.80	0.10	1.19	0.97	0.95	0.25	1.58	1.00	1.06	7.32
	0.85	0.99	1.02	0.72	1.10	1.06	1.03	1.13	1.09	1.07
	0.90	1.07	1.07	1.07	1.12	1.12	1.12	1.13	1.13	1.13
	0.95	1.05	1.06	1.06	1.07	1.08	1.08	1.08	1.08	1.08
	1.00	1.00	1.00	1.00	1.00	1.00	1.00	1.00	1.00	1.00
j/j_2	0.75	0.43	0.34	0.36	0.37	0.43	0.31	0.36		0.06
	0.80	0.43	0.42	0.44	0.41	0.44	0.41	0.41	0.42	0.23
	0.85	0.50	0.51	0.52	0.50	0.50	0.50	0.50	0.50	0.50
	0.90	0.62	0.62	0.62	0.62	0.62	0.62	0.62	0.62	0.62
	0.95	0.78	0.78	0.78	0.78	0.78	0.78	0.78	0.79	0.79
	1.00	1.00	1.00	1.00	1.00	1.00	1.00	1.00	1.00	1.00

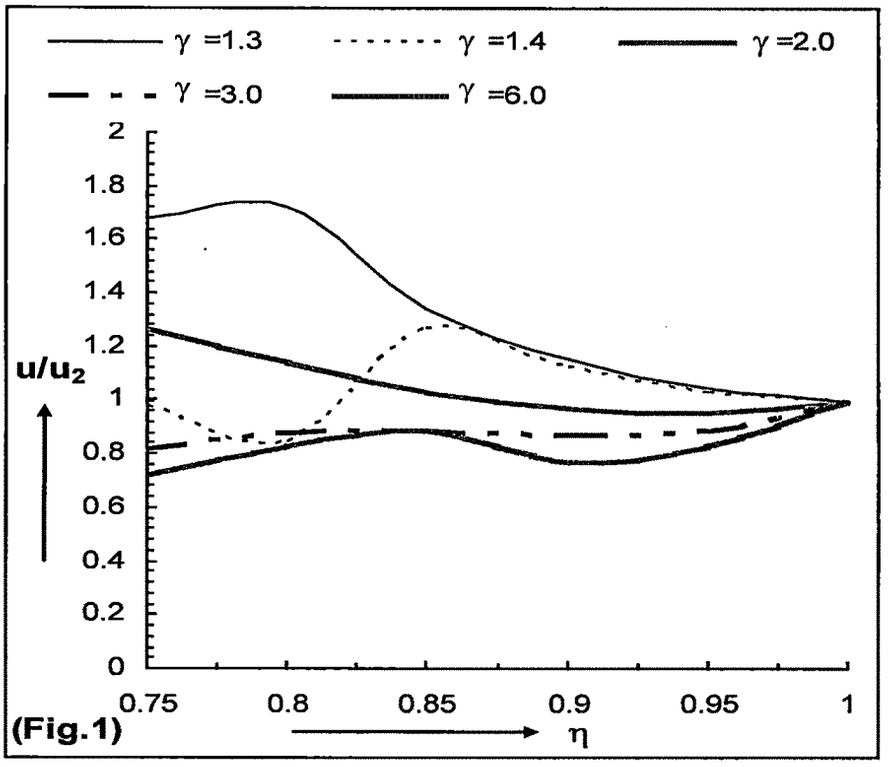

Fig. 1. The variation of velocity (u/u_2) behind the shock with similarity parameter η at k_p=0.1 and G=1.0 for variousγ.

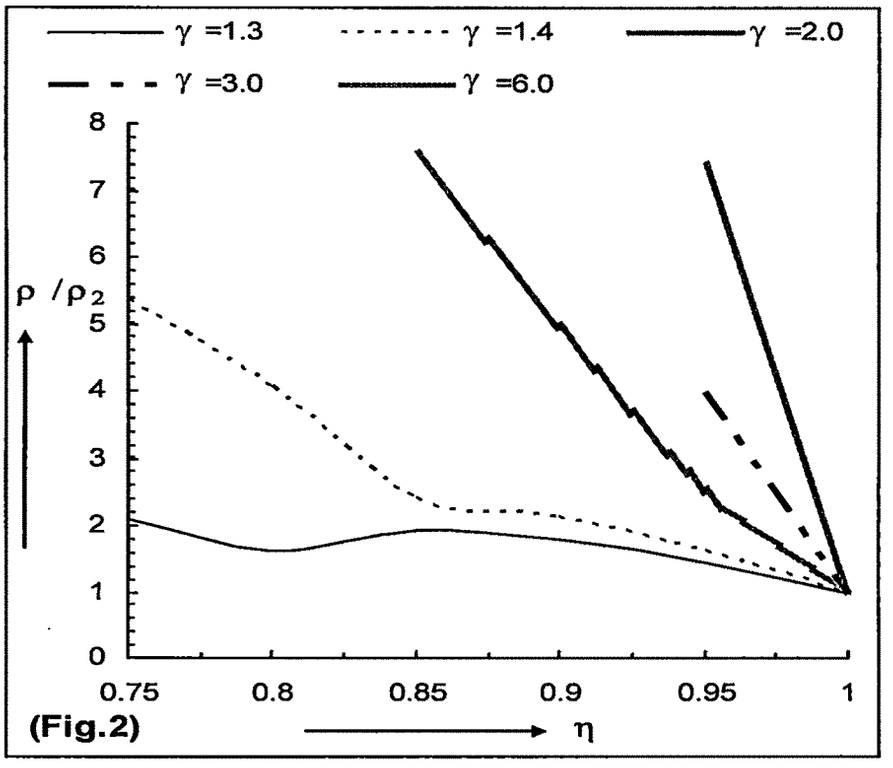

Fig. 2. The variation of density (ρ/ρ_2) behind the shock with similarity parameter η at k_p=0.1 and G=1.0 for variousγ.

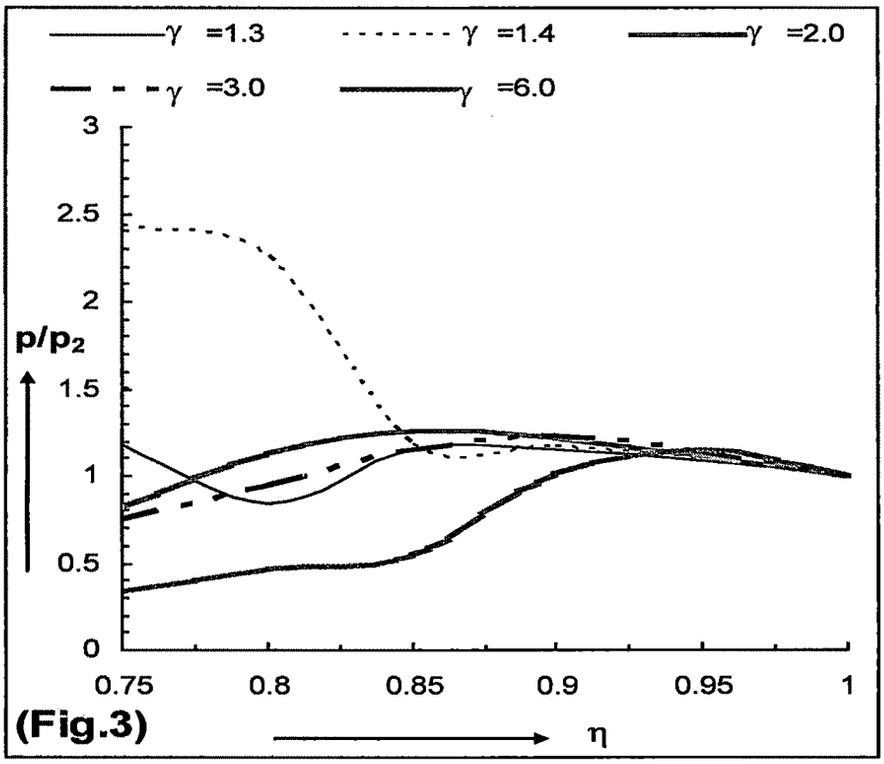

Fig. 3. The variation of pressure (p/p_2) behind the shock with similarity parameter η at k_p=0.1 and G=1.0 for variousγ.

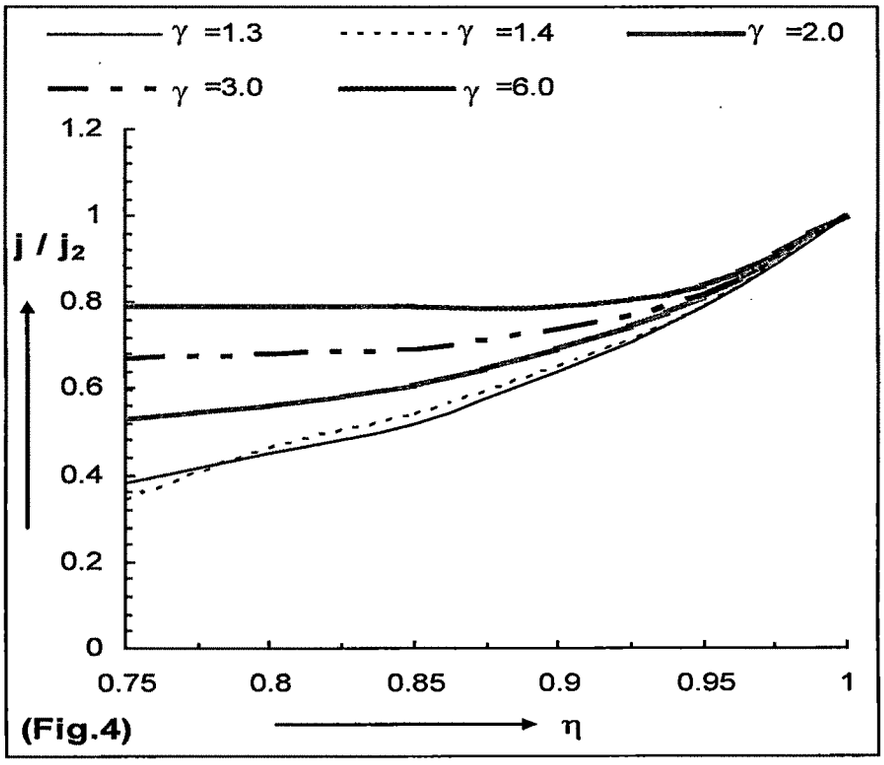

Fig. 4. The variation of monochromatic radiation (j/j_2) behind the shock with similarity parameter η at k_p=0.1 and G=1.0 for variousγ.

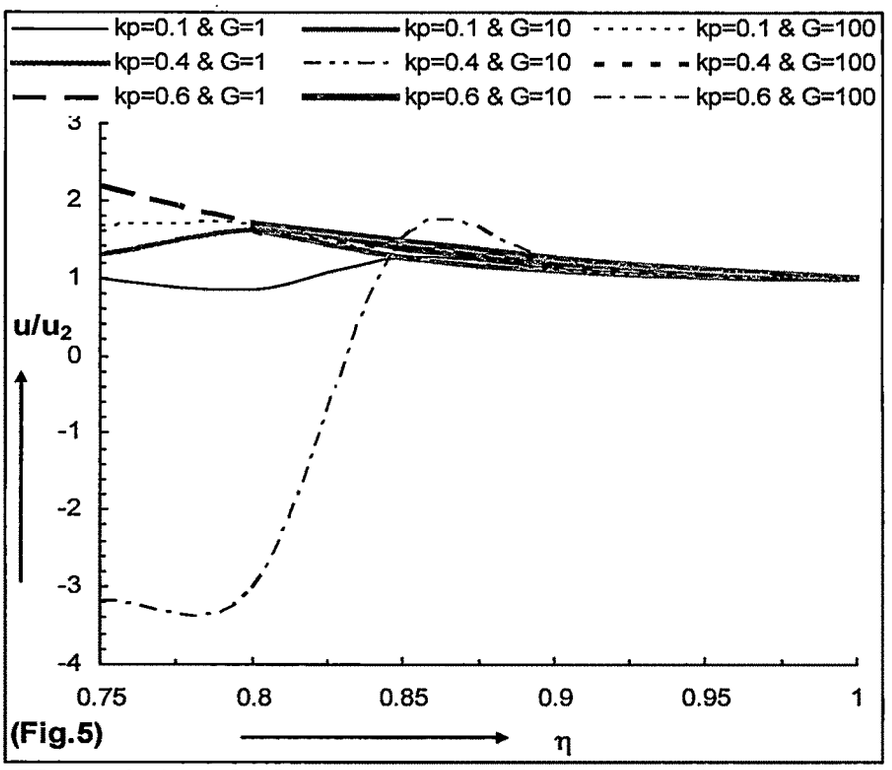

Fig. 5. The variation of velocity (u/u_2) behind the shock with similarity parameter η at $\gamma = 1.4$ for various k_p and G.

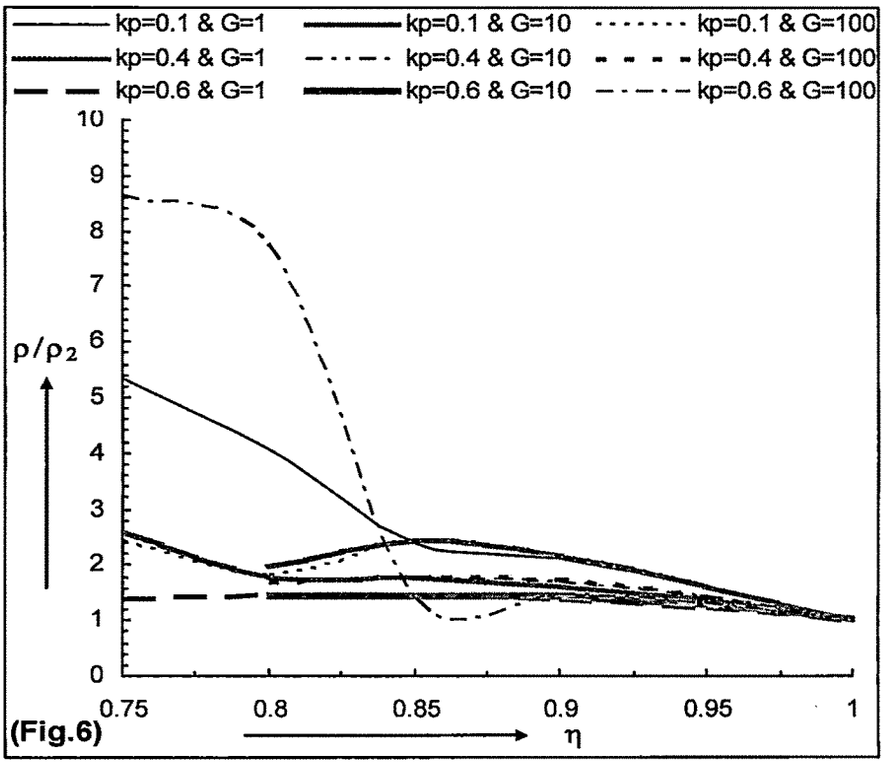

Fig. 6. The variation of density (ρ/ρ_2) behind the shock with similarity parameter η at $\gamma = 1.4$ for various k_p and G.

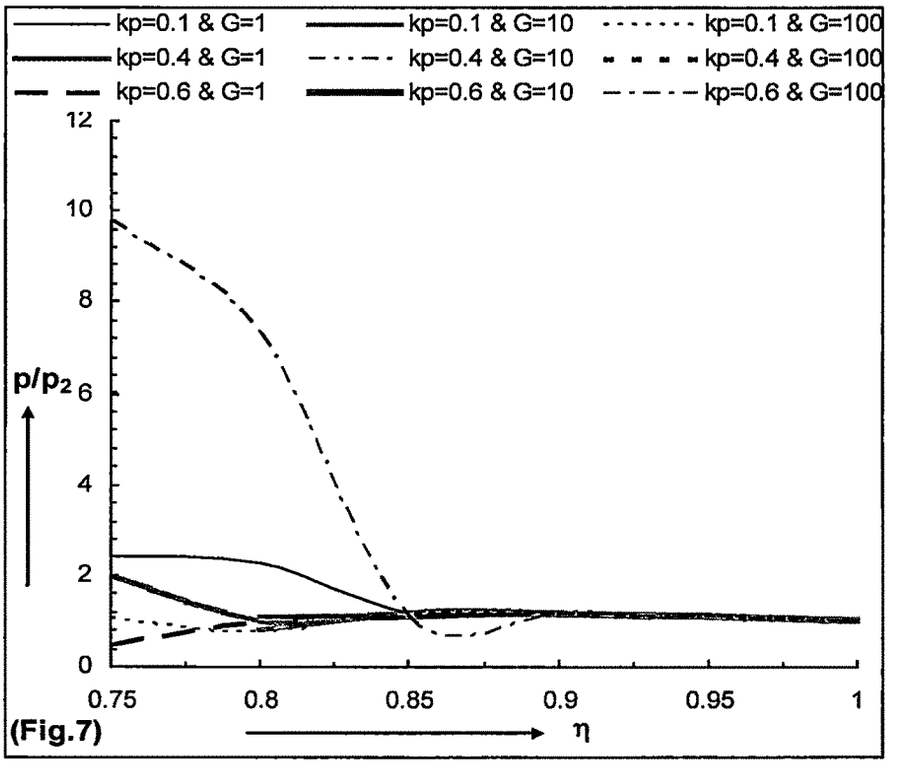

Fig. 7. The variation of pressure (p/p_2) behind the shock with similarity parameter η at $\gamma = 1.4$ for various k_p and G.

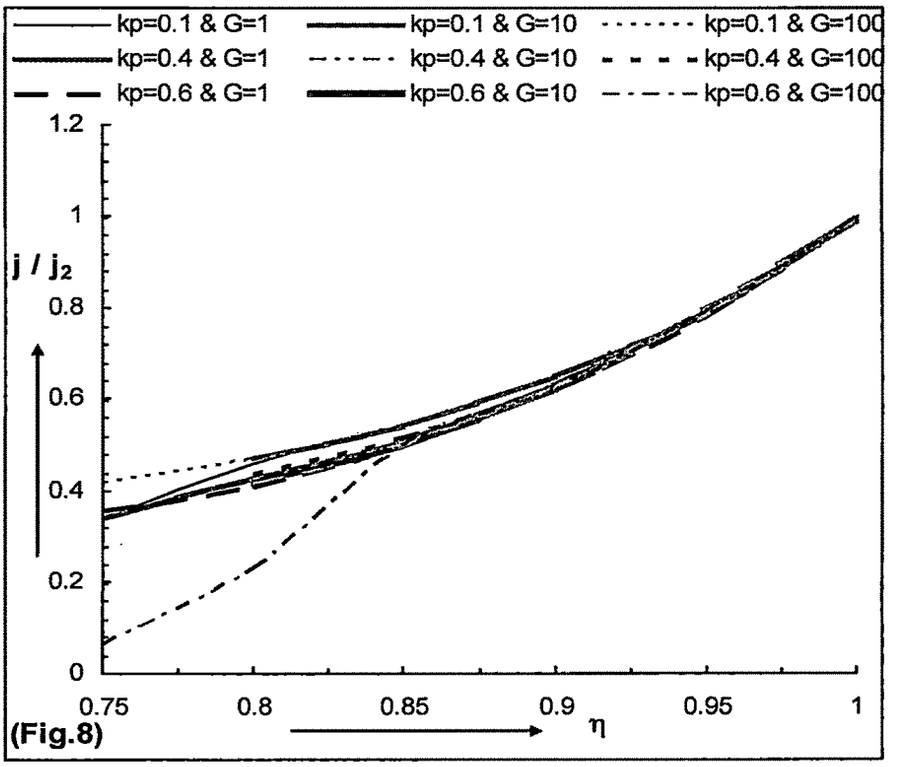

Fig. 8. The variation of monochromatic radiation (j/j_2) behind the shock with similarity parameter η at $\gamma = 1.4$ for various k_p and G

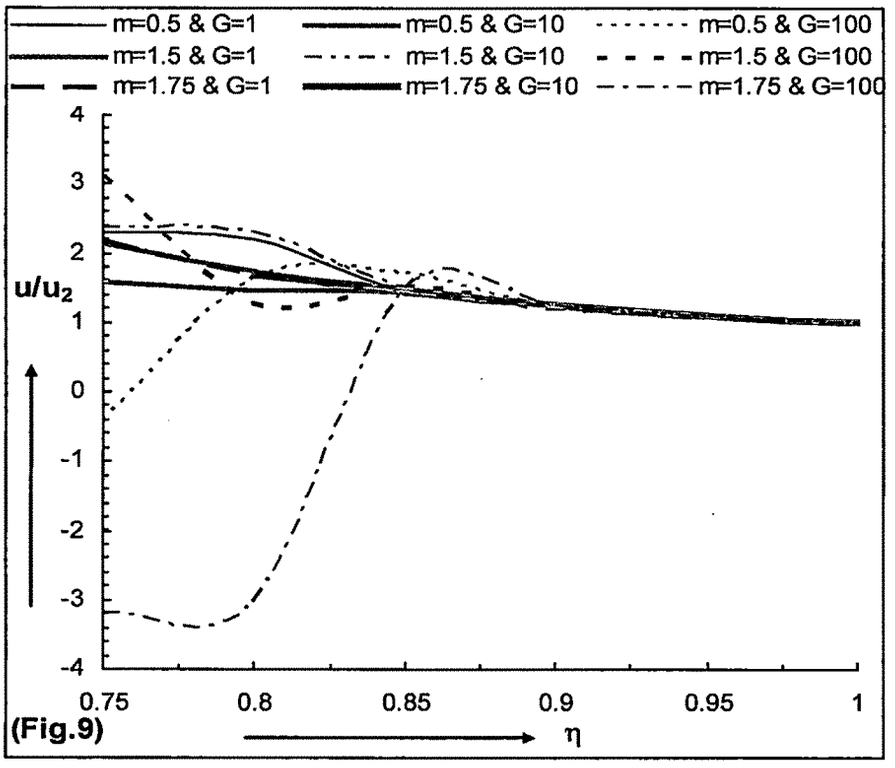

Fig. 9. The variation of velocity (u/u_2) behind the shock with similarity parameter η at $\gamma = 1.4$ and $k_p = 0.6$ for various m and G.

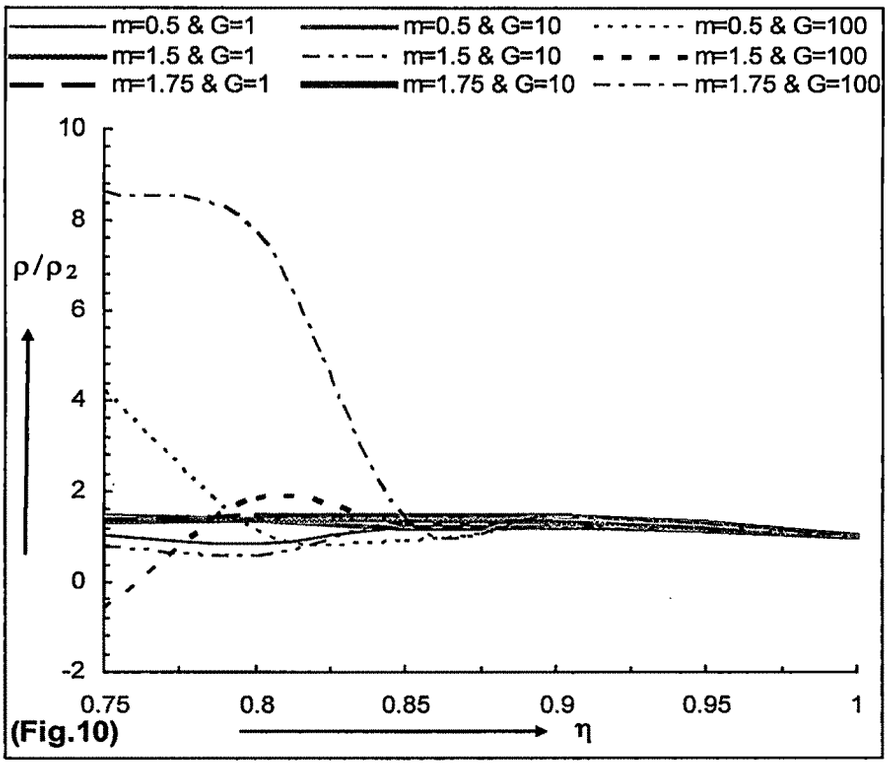

Fig. 10. The variation of density (ρ/ρ_2) behind the shock with similarity parameter η at $\gamma = 1.4$ and $k_p = 0.6$ for various m and G.

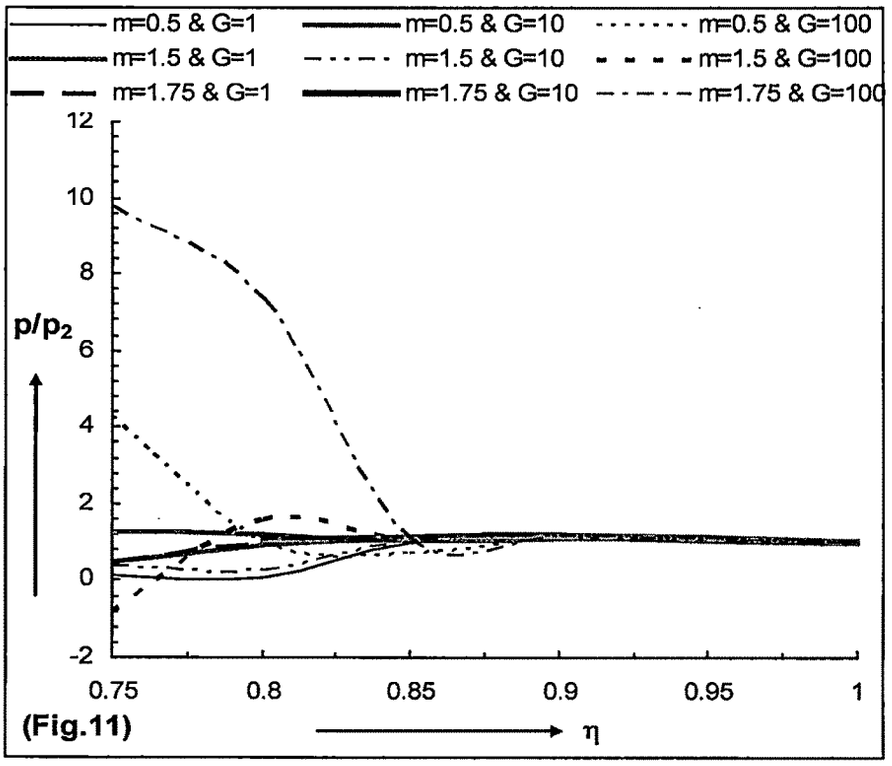

Fig.11. The variation of pressure (p/p_2) behind the shock with similarity parameter η at $\gamma = 1.4$ and $k_p = 0.6$ for various m and G.

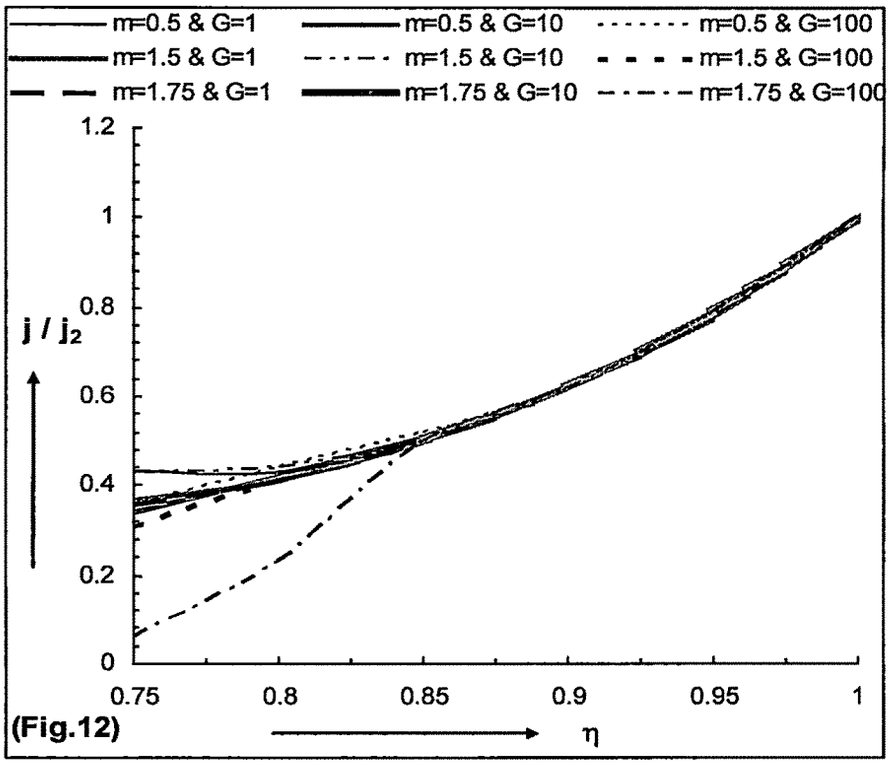

Fig.12.The variation of monochromatic radiation (j/j_2) behind the shock with similarity parameter η at $\gamma = 1.4$ and $k_p = 0.6$ for various m and G.

COMPUTER PROGRAM

```
#include<stdio.h>
#include<math.h>
#include<conio.h>
float sm_gama=1.4;
float H = -0.05;
float kp=0.6;
float beta_dash=1.0;
float alfa=5.0;
float m=1.75;
float g=1000.0;
float lem=(2.0+m)/5.0;
float delta=kp/(1.0-kp);
float gama=(sm_gama+delta*beta_dash)/(1.0+delta*beta_dash);
float z=kp/(g*(1.0-kp)+kp);
float beta=(gama-1.0+2.0*z)/(gama+1.0);
float f1(float u,float p,float d,float j,float x)// u-desh
{
float t11,t12,t13,t14,t17,t18,t19,t20,t21,num,deno,l;
l=(1.0/d)+(z/(1.0-z*d))+((gama-1.0)/((1.0-z*d)*d));
t11=-2.0*(u-1)/d;
t12=(lem-u)/p;
t13=-u*(u-1)-((2.0*p)/d);
t14=-3.0*l*u;
t17=p/x;
t18= 5.0*j+(alfa*x*pow(d,-0.5)*pow(p,1.5)*j*x);
t19=(gama-1);
t20=d*p*(1-z*d);
t21=(t18*t19)/t20;
deno=(l*p)-((lem-u)*(lem-u));
num=(t11+t13*t12+t14+t21)*t17 ;
return(num/deno);
}
float f2(float u,float p,float d,float j, float x) //p-desh
{
float t21,t22,t23;

t21=(lem-u)*d*f1(u,p,d,j,x);
t22=(d/x)*u*(u-1.0)+((2.0*p)/x);
t23=(t21-t22);
return(t23);
}
float f3(float u,float p,float d,float j,float x) //d-desh
{
float t31,t32,t33;
t31=(d/(lem-u));
t32=((3.0*u)/x)+f1(u,p,d,j,x);
```

```
t33=(t31*t32);
return(t33);
}

float f4(float p,float d,float j,float x)   //j-desh
{
float t41;
t41=alfa*x*pow(d,-0.5)*pow(p,1.5)*j;
return(t41);
}
main()
{
clrscr();
float x=1.0;
float u=1.0;
float p=1.0;
float d=1.0;
float j=1.0;

float k11,k21,k31,k41;
float k12,k22,k32,k42;
float k13,k23,k33,k43;
float k14,k24,k34,k44;
printf("kp=%1.2f m=%1.2f g=%1.2f gama=%1.2f beta=%1.2f delta=%1.2f \n
",kp,m,g,gama,beta,delta);
puts("-----------------------------------------------------------");
printf(" x       u      p     d     j    \n");
puts("-----------------------------------------------------------");
while (x > 0.7)
{
if(x<=1.0)
{
printf("%3.2f\t  %3.2f\t %3.2f\t %3.2f\t%3.2f\t \t\n",x,u,p,d,j);

}

k11=H*f1(u,p,d,j,x);
k21=H*f2(u,p,d,j,x);
k31=H*f3(u,p,d,j,x);
k41=H*f4(p,d,j,x);



k12=H*f1(u+0.5*k11,p+0.5*k21,d+0.5*k31,j+0.5*k41,x+0.5*H);
k22=H*f2(u+0.5*k11,p+0.5*k21,d+0.5*k31,j+0.5*k41,x+0.5*H);
k32=H*f3(u+0.5*k11,p+0.5*k21,d+0.5*k31,j+0.5*k41,x+0.5*H);
k42=H*f4(p+0.5*k21,d+0.5*k31,j+0.5*k41,x+0.5*H);
```

```
k13=H*f1(u+0.5*k12,p+0.5*k22,d+0.5*k32,j+0.5*k42,x+0.5*H);
k23=H*f2(u+0.5*k12,p+0.5*k22,d+0.5*k32,j+0.5*k42,x+0.5*H);
k33=H*f3(u+0.5*k12,p+0.5*k22,d+0.5*k32,j+0.5*k42,x+0.5*H);
k43=H*f4(p+0.5*k22,d+0.5*k32,j+0.5*k42,x+0.5*H);


k14=H*f1(u+k13,p+k23,d+k33,j+k43,x+H);
k24=H*f2(u+k13,p+k23,d+k33,j+k43,x+H);
k34=H*f3(u+k13,p+k23,d+k33,j+k43,x+H);
k44=H*f4(p+k23,d+k33,j+k43,x+H);

u+=(1.0/6.0)*(k11+2.0*k12+2.0*k13+k14);
p+=(1.0/6.0)*(k21+2.0*k22+2.0*k23+k24);
d+=(1.0/6.0)*(k31+2.0*k32+2.0*k33+k34);
j+=(1.0/6.0)*(k41+2.0*k42+2.0*k43+k44);
x+=H;
}
getch();
}
```